Conductivity Tomography for Non-Destructive Evaluation Using Pulsed Eddy Current With HTS SQUID Magnetometer

Hans-Joachim Krause, Grigory I. Panaitov, and Yi Zhang

***Abstract*—In standard eddy current nondestructive evaluation, the depth of investigation is restricted to a limited range around the skin depth of the chosen excitation frequency. We developed a pulsed eddy current NDE technique which allows simultaneous analysis of the sample at all depths. The advantage of SQUID magnetometers over induction coil sensors is that the field does not decay as rapidly as its time derivative, allowing for a broader range of investigated depths. Using rectangular excitation pulse trains, eddy currents are induced in the samples. The generated magnetic response field is recorded in off-time between the transmitter pulses by an HTS SQUID magnetometer. The early time data of the transient signal corresponds to the upper layers of the sample, while the late time data deliver information from deep layers. The transient responses are averaged over a number of alternating excitation pulses in order to enhance the signal-to-noise ratio and to eliminate drift. Scan measurements of different aluminum samples are presented. From the measured data, a 3D apparent conductivity image of the sample is calculated by applying a technique known from geophysical data interpretation. From this tomographic conductivity image of the sample, the position and depth of flaws in the material is readily determined.**

***Index Terms*—Pulsed eddy current, SQUID, tomography.**

I. Introduction

EDDY current testing is one of the most common techniques for Non-Destructive Evaluation (NDE) of metallic materials [1], [2]. Usually, eddy currents are induced at a single excitation frequency. Consequently, the response signal only contains information from depths down to about the standard penetration depth, $\delta = 1/\sqrt{\pi\sigma\mu f}$, with f denoting the frequency and σ and μ the electrical conductivity and permeability of the material, respectively. It is difficult to obtain selective information on structures at a given examination depth by analyzing the phase information of the response signal [3]. Using a pulsed eddy current (PEC) technique, this difficulty may be overcome [4].

The excitation pulse can be considered as a large number of single sinusoidal tests at various frequencies, each corresponding to a different standard penetration depth. When analyzing a single pulse response, one can get information from shallow layers (high frequency signal components) and from deep layers (low frequency components) simultaneously.

Manuscript received August 5, 2002. This work was supported in part by the German BMBF under Grant 13N7429/0.

The authors are with the Institute of Thin Films and Interfaces, Research Center Jülich GmbH, 52425 Jülich, Germany (e-mail: h.-j.krause@fz-juelich.de).

Digital Object Identifier 10.1109/TASC.2003.813688

Conventional PEC techniques use induction coil sensors which measure the derivative of the magnetic field, i.e., $\partial B/\partial t$. The field derivative decays much faster and, therefore, reaches the noise level much earlier than the transient of the B-field itself. This means that, compared to a coil, a magnetometer sensor potentially can record the transient data at later times.

It has been demonstrated that PEC testing using a Superconducting Quantum Interference Device (SQUID) is feasible [5]. However, a lock-in technique which is used in single frequency eddy current testing in order to improve the signal-to-noise (S/N) ratio [6], cannot be applied in pulsed eddy current. High-performance pulsed eddy current testing requires a data acquisition technique with an effective cancellation of the environmental noise and of low frequency, quasiconstant, signal drift. Recently, we have conducted PEC experiments for NDE of metals with a High Temperature Superconductor (HTS) SQUID in conjunction with a commercial LAPTEM® (Geoinstruments, Ltd.) data acquisition unit [7]. We demonstrated that, in the case of absolute coil excitation, the recorded PEC data may be inverted, using the formula for the impulse response of a homogeneous half-space [8], to obtain quasitomographic images of the so-called apparent conductivity of the medium [9].

In this paper, we present new experiments and extended features of the tomographic analysis of SQUID PEC data, especially the application to the case of differential excitation.

II. Experimental

The measurement principle is as follows: a square wave excitation current of alternating polarity with intermediate current-off-times is fed to an excitation coil located above the sample under test. Directly above the excitation coil, a SQUID magnetometer measures the magnetic field above the sample. The experimental setup is shown schematically in Fig. 1.

The samples consisted of stacked aluminum plates with 1.5 mm thickness. Two types of cracks, a long one and a small crack of 10 mm length, were used to investigate the transient signal of the flaw at different depths.

An HTS radio-frequency (rf) SQUID with a coplanar resonator [10] in a liquid nitrogen bath cryostat is positioned as close as possible to the coil and the sample. The SQUID is inductively coupled to a readout electronics with microprocessor-controlled automatic adjustment of the working point. The slew rate of the magnetometer is high enough ($\sim$2 mT / s) to follow the very sharp variations of the excitation field.

A commercial data acquisition unit LAPTEM was used to supply the excitation current and to synchronously record the

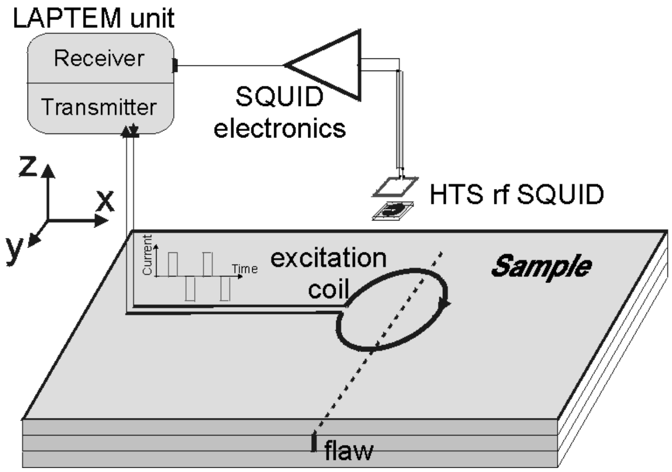

Fig. 1. Setup of the pulsed eddy current transient measurements using a SQUID sensor. The LAPTEM transmitter generates a square wave excitation current. During the excitation off time, the transient magnetic field response is measured by the SQUID and stacked in the receiver.

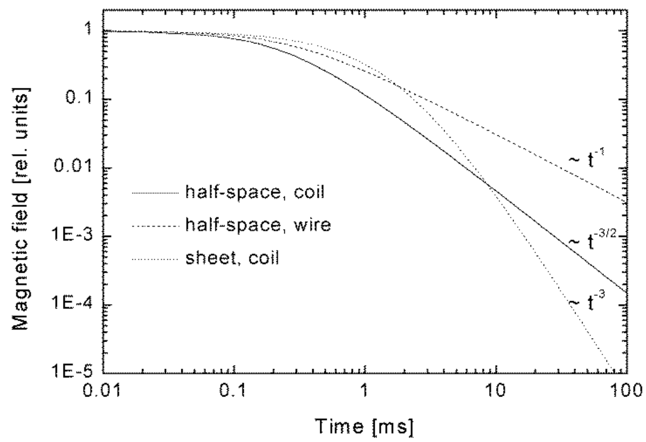

Fig. 2. Normalized magnetic field response as a function of time after current-off, calculated using (1) for absolute coil excitation, (2) for wire excitation of a homogeneous half-space, and (3) for absolute coil excitation of a sheet. Parameters of the calculations: conductivity $\sigma = 20$ MS/m, coil radius $a = 1$ cm, lateral displacement from wire $y = 1$ cm, plate thickness $d = 1$ cm, offset $z_0 = 1$ cm. The late-time decay exponent is indicated.

transient magnetic field response from the sample (bandwidth >40 kHz). This unit, designed for geophysical exploration using the Transient Electro-Magnetics (TEM) technique, performs stacking of several alternating measurements synchronously to the power line frequency. Thus, power line interference and low-frequency drift are efficiently suppressed.

Two types of excitation coils were used: an absolute coil, inducing circular currents in the sample, and a differential coil, which creates D-shaped currents in opposite directions. The advantage of a differential coil is that the excitation field in the middle of the coil is minimum, and the sensor device, being placed at its center, does not require a large dynamic range, allowing stronger excitation currents.

It is known that for very short excitation pulses, a so-called 'run-on' effect has to be taken into account. As eddy currents in the sample are induced not only by pulse switch-off ramp but by the switch-on ramp as well, the field run-on and run-off induce eddy currents in opposite directions. If the pulse length is too short, these two signals may compensate each other. Recently, we showed that, under appropriate conditions, the 'run-on' effect may even lead to a sign reversal of the transient signal [11]. The pulse period therefore was chosen to be 20 ms.

III. Signal Analysis Technique

From geophysical literature [8], we obtained the formula for the impulse response of a homogeneous half-space upon pulsed excitation with an absolute coil lying on the surface. The vertical magnetic field (perpendicular to the half-space) at a time t after switching off a current I in the loop is given by:

$$B_z = \frac{It}{\sigma a^3}\left[\left(2\theta^2 a^2 - 3\right)\operatorname{erf}(\theta a) + \frac{6}{\pi}\theta a \exp\left(-\theta^2 a^2\right)\right] \quad (1)$$

with σ denoting the electrical conductivity of the half-space, a the coil radius, and $\theta = \sqrt{\sigma\mu_0/4t}$. In case of a differential excitation, the geometry at the center is best represented by the expression for a single wire excitation [8], yielding a field

$$B_z = \frac{I\mu_0}{2\pi y}\left[1 + \frac{1}{\theta^2 y^2}\left(\exp\left(-\theta^2 y^2\right) - 1\right)\right]. \quad (2)$$

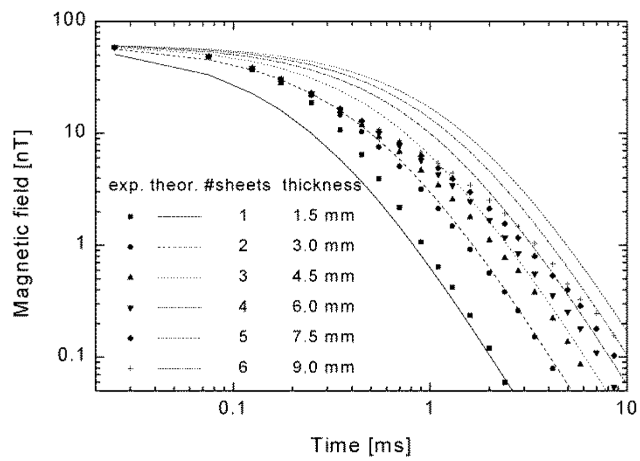

Fig. 3. Magnetic field response to a pulsed excitation with an absolute coil, measured on stacks of aluminum plates of different thickness (symbols). For comparison, the lines were calculated using (3).

Finally, the expression for the impulse response of an ideal sheet (thickness d, conductivity σ) to absolute coil excitation is given by [12]

$$B_z = \frac{I\mu_0}{2a} \cdot \left[\frac{a^2 + z_0^2}{a^2 + \left(z_0 + \left(2d\theta^2\right)^{-1}\right)^2}\right]^{3/2}. \quad (3)$$

The characteristic depth for a response at time t, the so-called diffusion depth [8], [12] is similar to the expression for the skin depth, (4), with $t = 1/f$. For different geometries, Fig. 2 depicts the decay with time, calculated using (1)–(3).

$$\delta = \sqrt{\frac{t}{\pi\mu_0\sigma}}. \quad (4)$$

IV. Measurements and Tomographic Analysis

A. Stack of Flawless Plates, Absolute Excitation

Using absolute coil excitation, stacks of $1, 2, \ldots 6$ aluminum plates (1.5 mm thickness each) were examined with the SQUID PEC. Fig. 3 shows the measured magnetic field responses.

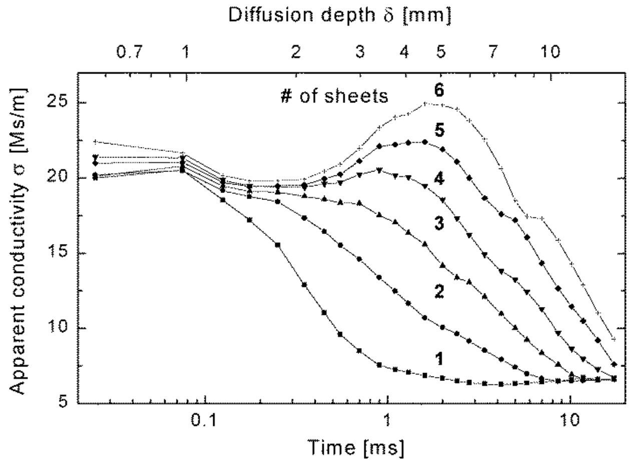

Fig. 4. Apparent conductivity σ of the sample, as derived using (3) from the measurement data depicted in Fig. 3.

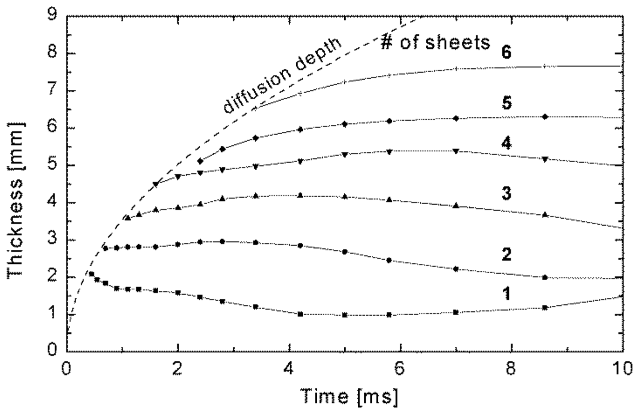

Fig. 5. Thickness d of the sample, as derived using (3) from the measurement data depicted in Fig. 3. The inversion data is valid only if the derived thickness is smaller than the diffusion depth for a given response time (dash).

The measured data were inverted by inserting the measured values in (1) and solving for the apparent conductivity, see Fig. 4. In conjunction with (4), the time scale is converted to a spatial scale, the diffusion depth. Note that for short times, the apparent conductivity approaches the real conductivity of 22 MS/m, independently measured by a calibrated meter. Steep decays of the apparent conductivity appear at values of δ close to the total thickness of the stacks, respectively.

When assuming that the conductivity is constant, (3) can alternately be solved for the thickness, see Fig. 5.

B. Stack of Plates With a Flaw, Absolute Excitation

Using absolute coil excitation, a stack of 4 aluminum plates (1.5 mm thickness each), with a large flaw (plate cut across) in one of the layers, was examined with the SQUID PEC system. All measured data and tomographic B-scan images of the apparent conductivity derived by inversion of (1) are found in [7]. As an example, Fig. 6 depicts the apparent conductivity image of the stack with the flaw in the second layer.C.

C. Stack of Plates With a Flaw, Differential Excitation

Using differential (double-D) coil excitation, a stack of 4 aluminum plates (total thickness 6 mm), with a 10 mm long crack in the fourth layer, was examined with SQUID PEC. The PEC measurements were recorded at every point of a 5 mm $\times$ 5 mm grid above the stack ($x = \pm 35$ mm, $y = \pm 45$ mm). Using (1), we corrected the data for time decay. For each different response time, corresponding to a different diffusion depth, we obtained a distinct quasitomographic C-scan image, see Fig. 7. These im-

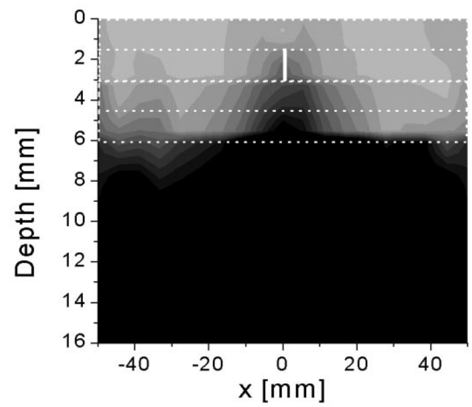

Fig. 6. Tomographic B-scan-image of the apparent electrical conductivity as a function of position and depth, for a sample of 4 stacked aluminum plates, with a crack in the second layer. White lines indicate contours of the sheets (dotted) and the crack (solid).

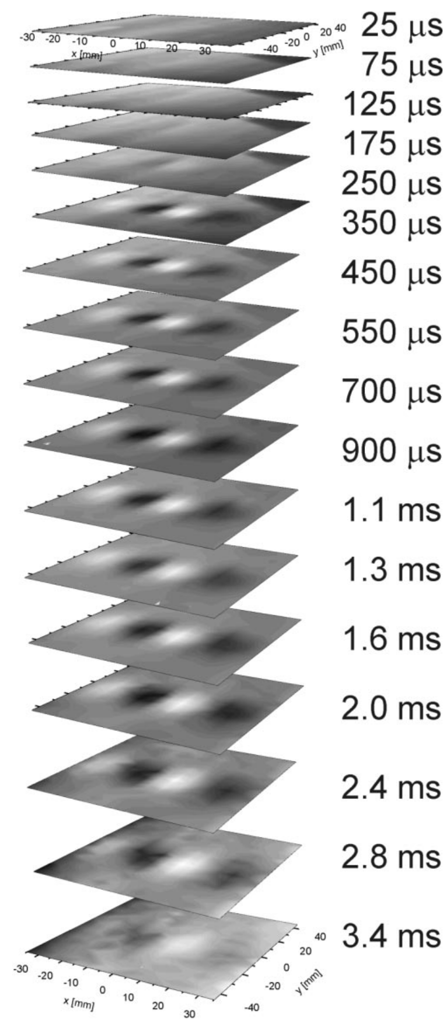

Fig. 7. Tomographic C-scan-images for different response times, corresponding to different diffusion depths.

ages may be interpreted as horizontal cuts of the sample at different depths. Similarly, B-scans have also been derived.

Even though the absolute value of the apparent conductivity may not be isolated due to the differential excitation, the images may be analyzed for deviations from homogeneity. A clear signature of the 10 mm long flaw, with a differential image at either crack end, appears at a response time of 350 μs and vanishes around 2.8 ms. These times correspond to diffusion depths of 2.1 and 6.0 mm, respectively. The real depth of the crack was from 4.5 to 6.0 mm. The tomographic data allows to locate the crack, however, the crack onset is underestimated.

V. Conclusion

We performed pulsed eddy current testing of metallic structures using an HTS SQUID magnetometer sensor in conjunction with absolute or differential coil excitation. It was shown that a signal analysis in analogy to inversion techniques known in geophysical exploration can be applied to PEC data of NDE samples. When using an absolute excitation coil, the spatial distribution of the sample's apparent electrical conductivity $\sigma(x, y, z)$ can be derived from the measured magnetic field transients. The obtained tomographic conductivity image of the sample allow to localize flaws in the material. When using a differential excitation, the tomographic inversion may also be applied, with the only drawback that the absolute quantity of apparent conductivity may not be derived. However, the crack position, orientation, length and depth may be extracted from the tomographic PEC data. This imaging feature might become a convenient tool for NDE inspectors as it simplifies the evaluation of their measurements.

References

[1] G. B. Donaldson, A. Cochran, and D. McA. McKirdy, "The use of SQUIDs for nondestructive evaluation," in *SQUID Sensors*, H. Weinstock, Ed. Dordrecht, The Netherlands: Kluwer, 1996, pp. 599–628.

[2] W. G. Jenks, S. S. H. Sadeghi, and J. P. Wikswo, "SQUIDs for nondestructive evaluation," *Journal of Physics*, vol. D 30, pp. 293–323, 1997.

[3] M. v. Kreutzbruck, M. Mück, and C. Heiden, "Simulations of eddy current distributions and crack detection algorithms for a SQUID based NDE system," in *Proceedings of the 7th European Conference on NDT*, B. Larsen, Ed., Broendby, 1998, pp. 2513–2520.

[4] R. A. Smith and G. R. Hugo, "Transient eddy-current NDE for ageing aircraft," *Insight*, vol. 43, no. 1, pp. 14–20, 2001.

[5] W. N. Podney and J. C. Moulder, "Electromagnetic microscope for deep, PEC inspections," in *Rev.Prog. QNDE*, D. O. Thompson and D. E. Chimenti, Eds. New York: Plenum Press, 1997, vol. 16, pp. 1037–1044.

[6] H.-J. Krause and M. v. Kreutzbruck, "Recent developments in SQUID NDE," *Physica C*, vol. 368, pp. 70–79, 2002.

[7] G. Panaitov, H.-J. Krause, and Y. Zhang, "Conductivity tomography based on pulsed eddy current with SQUID magnetometer," in *Rev. Prog. QNDE*, D. O. Thompson and D. E. Chimenti, Eds. Melville, NY: American Institute of Physics, 2002, vol. 21A, pp. 445–452.

[8] B. R. Spies and F. C. Frischknecht, "Electromagnetic sounding," in *EM Methods of Applied Geophysics*, M. Nabighian, Ed: Soc. Expl. Geophys., 1991, pp. 285–425.

[9] G. Panaitov, H. -J. Krause, and Y. Zhang, "Pulsed eddy current transient technique with HTS SQUID magnetometer for nondestructive evaluation," *Physica C*, vol. 372–376, pp. 278–281, 2002.

[10] Y. Zhang, "Evolution of HTS rf SQUIDs," *IEEE Trans. Appl. Supercond.*, vol. 11, no. 1, pp. 1038–1042, Mar. 2001.

[11] G. Panaitov, M. Bick, Y. Zhang, and H.-J. Krause, "Effect of repetitive-transmitter signals on SUID response in TEM," *IEEE Trans. Applied Supercond.*, vol. 11, no. 1, pp. 888–891, March 2001.

[12] M. N. Nabighian and J. C. Macnae, "Time domain electromagnetic prospecting methods," in *EM Methods of Applied Geophysics*, M. Nabighian, Ed: Soc. Expl. Geophys., 1991, pp. 427–520.